

HQSAR Study on Substituted 1H-Pyrazolo[3,4-b]pyridines Derivatives as FGFR Kinase Antagonists

Swapnil P. Bhujbal^{1*}, Pavithra K. Balasubramanian^{1*},
Seketoulie Keretsu¹, and Seung Joo Cho^{1,2†}

Abstract

Fibroblast growth factor receptor (FGFR) belongs to the family of receptor tyrosine kinase. They play important roles in cell proliferation, differentiation, development, migration, survival, wound healing, haematopoiesis and tumorigenesis. FGFRs are reported to cause several types of cancers in humans which make it an important drug target. In the current study, HQSAR analysis was performed on a series of recently reported 1H-Pyrazolo [3,4-b]pyridine derivatives as FGFR antagonists. The model was developed with Atom (A) and bond (B) connection (C), chirality (Ch), hydrogen (H) and donor/acceptor (DA) parameters and with different set of atom counts to improve the model. A reasonable HQSAR model ($q^2=0.701$, SDEP=0.654, NOC=5, $r^2=0.926$, SEE=0.325, BHL=71) was generated which showed good predictive ability. The contribution map depicted the atom contribution in inhibitory effect. A contribution map for the most active compound (compound 24) indicated that hydrogen and nitrogen atoms in the side chains of ring B as well as hydrogen atoms in the side chain of ring C and the nitrogen atom in the ring D contributed positively to the activity in inhibitory effect whereas, the lowest active compound (compound 04) showed negative contribution to inhibitory effect. Thus results of our study can provide insights in the designing potent and selective FGFR kinase inhibitors.

Keywords: FGFR Kinase, HQSAR, Pyridine Derivatives, FGFR Kinase Inhibitors

1. Introduction

Fibroblast growth factor receptors (FGFRs) comprise a family of four highly conserved transmembrane receptor tyrosine kinases (FGFR1-4)^[1,2]. They consist of three extracellular Ig-like domains (D1-D3), connected by flexible linker sequences, a single transmembrane helix domain and a cytoplasmic region that harbors a conserved tyrosine kinase domain^[1]. Recently, the fibroblast growth factor receptor like 1 (FGFR1 or FGFR5) a fifth member of the FGFR family has been discovered, that exhibit three extracellular Ig-like domains but lacks the protein tyrosine kinase domain^[1,3]. The major survival and proliferative signaling pathways are triggered due to receptor activation by

FGFs that initiates a cascade of intracellular events^[2]. The FGFs play important roles in development, wound healing, tumorigenesis and hematopoiesis^[1,2]. In the recent studies it has been stated that FGFRs play a role in cancer by inducing cancer cell proliferation, survival and angiogenesis^[1].

Frequent deregulation of the FGFR/FGF system occurs in human cancers^[4]. Ligand-dependent or independent mechanisms are responsible of the abnormal activation of FGFR signaling^[5]. Ligand independent mechanisms involve activating FGFR mutations and FGFR overexpression due to chromosomal translocation, gene amplification, aberrant transcriptional regulation or down-modulation of negative regulators. The paracrine or autocrine production of FGFs proteins by stromal or tumor cells leads to ligand-dependent abnormal activation of FGFR signaling^[1,6,7]. FGFR undergoes dimerization and autophosphorylation upon FGF binding, resulting in activation of downstream signaling pathways, such as the MAPK and PLC γ pathways^[8-12]. The most commonly affected cancers from FGFR aberrations include urothelial cancer (32%), breast cancer

¹Department of Biomedical Sciences, College of Medicine, Chosun University, Gwangju 501-759, Korea

²Department of Cellular Molecular Medicine, College of Medicine, Chosun University, Gwangju 501-759, Korea

*Authors have contributed equally to this work

†Corresponding author : chosj@chosun.ac.kr

(Received : May 1, 2017, Revised : June 15, 2017,

Accepted : June 25, 2017)

(18%), squamous lung cancer (~13%), endometrial cancer (~13%) and ovarian cancer (~9%)^[1].

Many small molecules which are reported to target FGFR have been in clinical development, such as dovitinib, nintedanib and cediranib^[13,14]. Nevertheless, most of these compounds have multitarget specificity which leads to unexpected side effects in their anticancer therapies^[15,16]. Currently, several selective FGFR inhibitors have progressed into clinical trials, such as NVP-BGJ398, AZD4547 and CH5183284^[14]. PD173074 is the first reported selective FGFR inhibitor, while inhibiting PDGFR, c-Src and EGFR, as well as few serine/threonine kinases^[14]. Hence it is pivotal to design

potent and selective FGFR inhibitors. In the present work, Hologram QSAR (HQSAR) was used to develop a model to identify the vital group or atom that caused inhibition of FGFR. Our result could be helpful to design novel and unique FGFR inhibitors.

2. Methodology

2.1. Dataset

A series of Substituted 1H-Pyrazolo[3,4-b]pyridines reported as potent FGFR kinase inhibitors (29 compounds) were taken for the HQSAR study^[17] and were shown in Table 1. All the 29 structures were sketched

Table 1. Structure and biological activity values of substituted 1H-Pyrazolo[3,4-b]pyridines as FGFR kinase inhibitors

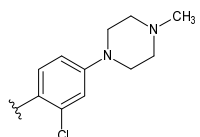
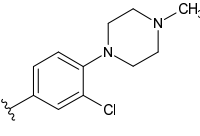
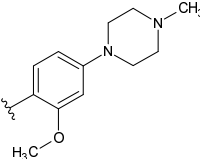
Compounds 1-4				Compounds 5-29	
Compound	X	Y	R ¹	R ²	pIC ₅₀
1	H	N	H	-	5.431
2	Cl	N	H	-	9.523
3	Cl	CH	H	-	8.482
4	Cl	N	Me	-	5.301
5	-	-	-		7.854
6	-	-	-		7.839
7	-	-	-		7.128

Table 1. Continued

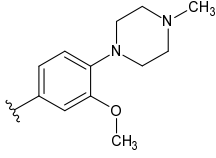
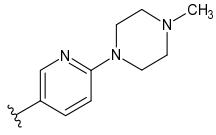
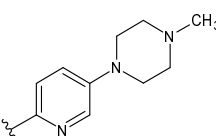
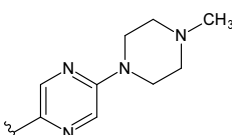
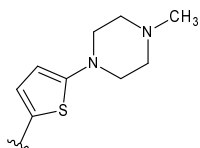
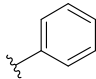
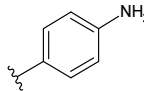
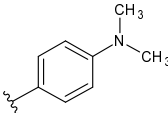
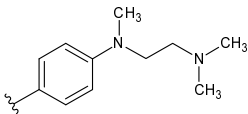
Compound	X	Y	R ¹	R ²	pIC ₅₀
8	-	-	-		7.848
9	-	-	-		8.208
10	-	-	-		8.108
11	-	-	-		7.979
12	-	-	-		8.387
13	-	-	-		7.373
14	-	-	-		8.056
15	-	-	-		7.783
16	-	-	-		8.409

Table 1. Continued

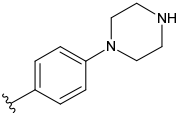
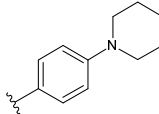
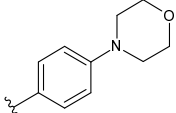
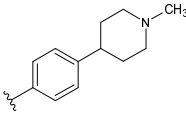
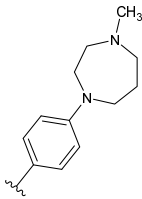
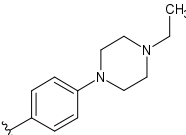
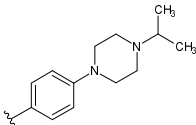
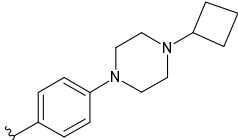
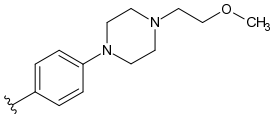
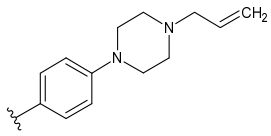
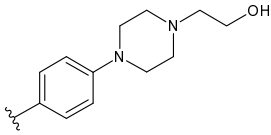
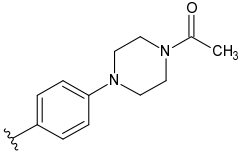
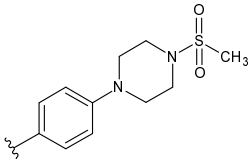
Compound	X	Y	R ¹	R ²	pIC ₅₀
17	-	-	-		7.932
18	-	-	-		8.056
19	-	-	-		8.114
20	-	-	-		8.161
21	-	-	-		8.143
22	-	-	-		9.301
23	-	-	-		8.854
24	-	-	-		9.699
25	-	-	-		9.523

Table 1. Continued

Compound	X	Y	R ¹	R ²	pIC ₅₀
26	-	-	-		9.222
27	-	-	-		9.523
28	-	-	-		9.523
29	-	-	-		9.699

and optimized by energy minimization with tripos force field using SYBYL-X 2.1^[18]. Gasteiger-Hückel charges were applied as partial charges. The biological data expressed as IC₅₀ values were converted into pIC₅₀ (-log IC₅₀) values. The values span 4.3 log units which indicate the dataset is adequate for a QSAR study. The dataset was then used for HQSAR analysis.

2.2. HQSAR

HQSAR provides the ability to generate QSAR models of high statistical quality and predictive value rapidly. It does not require a 3D structure of molecules or molecular alignments. Instead, HQSAR model development uses 2D structure directed fragment fingerprint. Based on the hologram length (HL) parameter given, these molecular fingerprints are broken into strings at fixed intervals. The HL determines the number of bins in the hologram into which the fragments are hashed. The optimal HQSAR model was derived from screening through the 12 default HL values, which were a set of 12 prime numbers ranging from 53-401. The model

development was performed using the following parameters: atom (A), bond (B), connection (C), chirality (Ch), hydrogen (H) and donor/acceptor (DA). The validity of the model depends on statistical parameters such as r^2 , q^2 by LOO^[19].

3. Results and Discussion

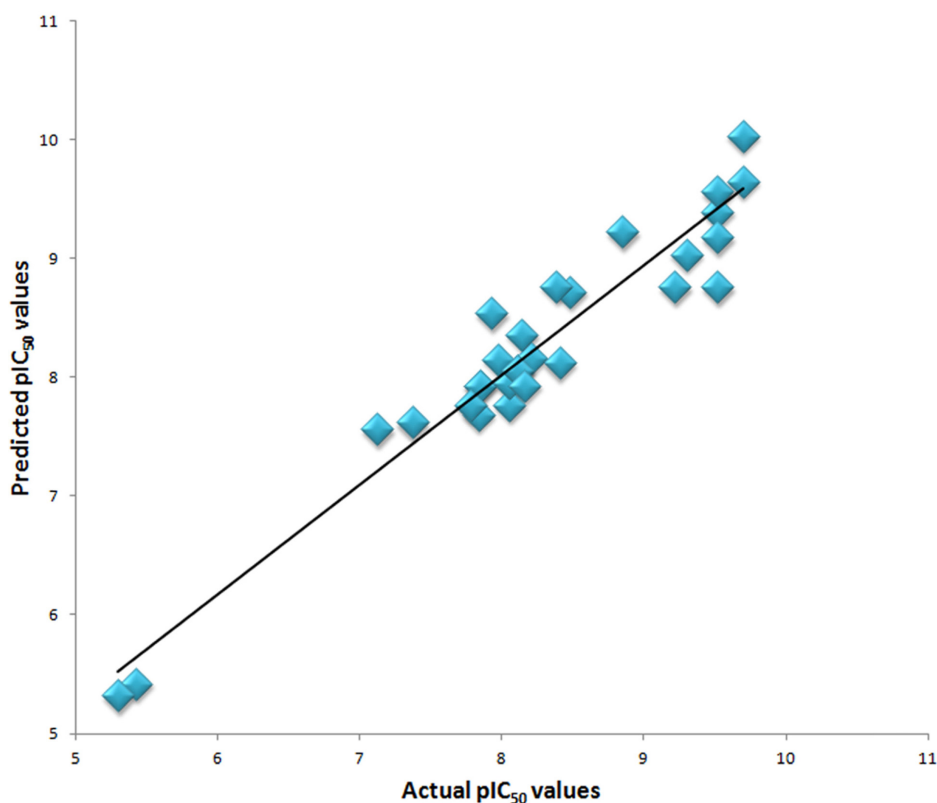
3.1. HQSAR Analysis

The HQSAR model with reasonable predictive ability with regard to q^2 and r^2 was generated. Atom (A) and bond (B) connection (C), chirality (Ch), hydrogen (H) and donor/acceptor (DA) parameters with different hologram lengths were used to develop models. Among all, the model with C/Ch/DA combination showed a q^2 of 0.701 and an r^2 of 0.926 with 0.654 as standard error of prediction and 0.325 as standard error of estimate. The statistical values of the model obtained were found to be satisfactory and are summarized in Table 2. The actual and predicted activity values for the selected model are given in Table 4. The scatter plot for the

Table 2. HQSAR models with different statistical parameters

Model	Fragment distinction	NOC	q^2	SDEP	r^2	SEE	BHL
1.	A/C/DA	6	0.543	0.826	0.947	0.282	257
2.	C/Ch/DA	5	0.701	0.654	0.926	0.325	71
3.	A/B/C/H	2	0.093	1.071	0.308	0.935	71
4.	A/B/H/DA	2	0.305	0.938	0.577	0.732	61
5.	B/C/Ch/DA	6	0.594	0.779	0.948	0.280	61
6.	A/B/C/Ch/DA	6	0.459	0.899	0.924	0.336	53
7.	A/B/C/H/Ch	2	0.093	1.071	0.308	0.935	71
8.	A/B/C/H/DA	6	0.270	1.045	0.926	0.176	53
9.	A/B/C/H/DA/Ch	6	0.298	1.024	0.938	0.305	53

A=atom, B=bond, C=connection, H=hydrogen, Ch=chirality, DA=hydrogen bond donor/acceptor, NOC=number of components, q^2 =cross-validated correlation coefficient, SDEP=cross-validated standard error of prediction, r^2 =non-cross-validated correlation coefficient, SEE=standard error of estimate, BHL=best hologram length. Model selected to exploit atom count parameter is shown in bold face.

**Fig. 1.** Scatter plot diagram for HQSAR analysis. Plot shows the actual and predicted pIC₅₀ values of compounds.

same is depicted in Fig. 1. The highest q^2 value obtained for parameters C/Ch/DA was explored with an optional atom count (1-11) for further improvement of q^2 . The default atom count (4-7) gave the best statistical model

(Table 3). A standard color coding system was used to indicate atomic contributions in the HQSAR model (Fig. 2). A yellow, green-blue and green indicated favorable or positive contribution to the activity, while

Table 3. Statistical summary of C/Ch/DA model explored for the different atom counts

Atom Count	NOC	q^2	SDEP	r^2	SEE	BHL
1-4	5	0.544	0.807	0.903	0.373	83
2-5	4	0.648	0.694	0.913	0.344	71
3-6	6	0.632	0.742	0.947	0.283	199
4-7	5	0.701	0.654	0.926	0.325	71
5-8	5	0.590	0.766	0.925	0.328	199
6-9	5	0.627	0.730	0.906	0.366	53
7-10	3	0.428	0.867	0.751	0.572	53
8-11	5	0.357	0.959	0.929	0.318	199

Final model selected for HQSAR analysis is represented in bold.

Table 4. Actual pIC_{50} and predicted pIC_{50} with their residual values of selected HQSAR model

Compound	Actual pIC_{50}	CoMSIA	
		Predicted	Residual
1	5.431	5.422	0.008
2	9.523	8.761	0.762
3	8.482	8.722	-0.241
4	5.301	5.320	-0.019
5	7.854	7.927	-0.073
6	7.839	7.688	0.150
7	7.128	7.564	-0.435
8	7.848	7.933	-0.085
9	8.208	8.161	0.047
10	8.108	8.057	0.051
11	7.979	8.152	-0.173
12	8.387	8.770	-0.383
13	7.373	7.622	-0.249
14	8.056	7.770	0.286
15	7.783	7.770	0.012
16	8.409	8.124	0.285
17	7.932	8.542	-0.611
18	8.056	7.957	0.098
19	8.114	8.059	0.055
20	8.161	7.933	0.229
21	8.143	8.357	-0.214
22	9.301	9.031	0.270
23	8.854	9.228	-0.374
24	9.699	9.654	0.045
25	9.523	9.394	0.129
26	9.222	8.762	0.460
27	9.523	9.565	-0.042
28	9.523	9.179	0.344
29	9.699	10.033	-0.334

unfavorable and negative contribution to the activity was denoted by red, red-orange and orange. For the study of atomic contribution, molecules were selected based on their activity profile^[20-23].

All the dataset molecules had a common substructure and varied in X, Y, R¹, R² and R³ substructure. Fig. 2 shows atom contribution map for the most active compound (compound 24). It indicate that hydrogen and nitrogen atoms in the side chains of ring B contributed positively to the activity (pIC_{50} =9.699). Also the hydrogen atoms in the side chain of ring C and the nitrogen atom in the ring D contributed positively to the activity, whereas, the contribution map (Fig. 2) for the lowest active compound (compound 04) indicated that hydrogen atom in the side chain of ring C contributed negatively to the activity (pIC_{50} =5.301) with no positive contribution from the other atoms. We also have checked contribution in inhibitory effect for few compounds from active, medium active and low active profile. Compound 02 (pIC_{50} =9.523), which has the second highest activity showed positive contribution from hydrogen and oxygen atoms of side chains of ring C.

On the contrary, medium active compound 21 (pIC_{50} =8.413) showed positive contribution from hydrogen and oxygen atoms of side chains of ring C with negative contribution from chlorine and hydrogen atoms of side chains of ring A. Whereas, compound from low active series such as compound 01 (pIC_{50} =5.431) showed negative contribution from hydrogen and nitrogen atoms of ring D and showed no positive contribution from ring A and ring B. This might be the reason why these molecules exhibit low activity and have less inhibitory effect.

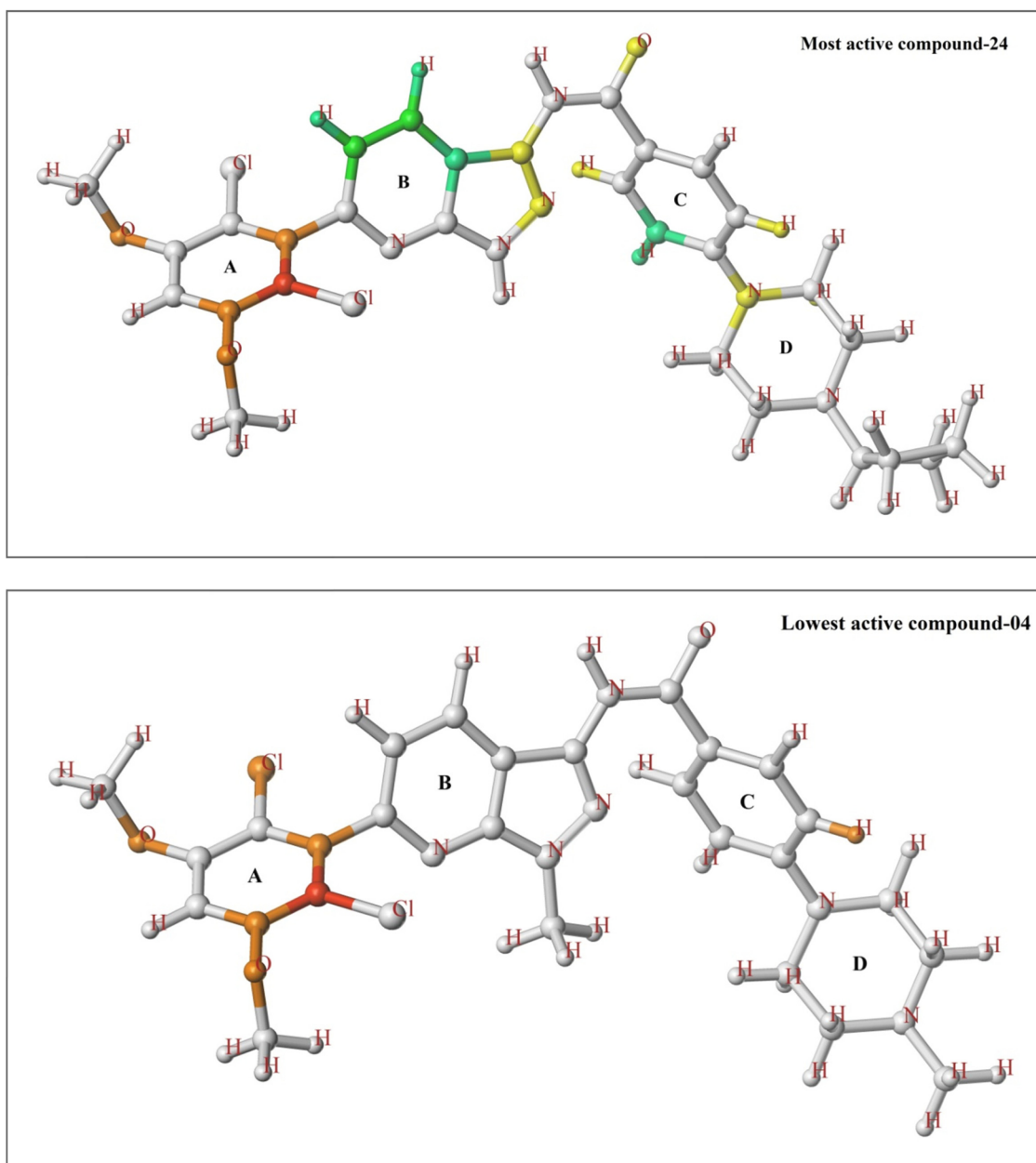


Fig. 2. HQSAR atomic contribution maps. Map is shown for highly active compound-24 and lowest active compound-04.

4. Conclusion

HQSAR is a contemporary 2D-QSAR technique, which needs only 2D structures with corresponding biological activity. HQSAR analysis illustrates the relationship of atom contribution to the activity of the

compounds. The positive atom contributions of compound are linked with its increased activity. Medium active compounds have intermediate contribution in the activity with negative contribution as well. Whereas, low active compounds showed negative contribution to the most and had no positive contribution to the inhib-

itory effect. Fragment analyses of HQSAR can be carried out as further work to avail the compound modification guidelines. This could be helpful to design novel active compounds. The presently-developed HQSAR model aids the identification of the functional groups and atoms and highlights their importance and contribution to inhibitory potency.

Acknowledgements

This work was supported by the National Research Foundation of Korea Grant funded by the Korean Government (NRF-2016R1D1A1B01007060).

References

- [1] A. D. Luca, D. Frezzetti, M. Gallo, and N. Normanno, "FGFR-targeted therapeutics for the treatment of breast cancer", *Expert Opin. Investig. Drugs*, Vol. 26, pp. 303-311, 2017.
- [2] I. S. Babina and N. C. Turner, "Advances and challenges in targeting FGFR signalling in cancer", *Nat. Rev. Cancer*, Vol. 17, pp. 318-332, 2017.
- [3] K. H. Tiong, L. Y. Mah, and C.-O. Leong, "Functional roles of fibroblast growth factor receptors (FGFRs) signaling in human cancers", *Apoptosis*, Vol. 18, pp. 1447-1468, 2013.
- [4] M. Touat, E. Ileana, S. Postel-Vinay, F. André, and J. C. Soria, "Targeting FGFR signaling in cancer", *Clin. Cancer Res.*, Vol. 21, pp. 2684-2694, 2015.
- [5] E. M. Haugsten, A. Wiedlocha, S. Olsnes, and J. Wesche, "Roles of fibroblast growth factor receptors in carcinogenesis", *Mol. Cancer Res.*, Vol. 8, pp. 1439-1452, 2010.
- [6] H. Greulich and P. M. Pollock, "Targeting mutant fibroblast growth factor receptors in cancer", *Trends Mol. Med.*, Vol. 17, pp. 283-292, 2013.
- [7] H. K. Ho, A. H. Yeo, T. S. Kang, and B. T. Chua, "Current strategies for inhibiting FGFR activities in clinical applications: opportunities, challenges and toxicological considerations", *Drug Discov. Today*, Vol. 9, pp. 51-62, 2014.
- [8] J. M. Siegfried, M. Farooqui, N. J. Rothenberger, S. Dacic, and L. P. Stabile, "Interaction between the estrogen receptor and fibroblast growth factor receptor pathways in non-small cell lung cancer", *Oncotarget*, Vol. 8, pp. 24063-24076, 2017.
- [9] E. M. Haugsten, A. Wiedlocha, S. Olsnes, and J. Wesche, "Roles of fibroblast growth factor receptors in carcinogenesis", *Mol. Cancer Res.*, Vol. 8, pp. 1439-1452, 2010.
- [10] Y. J. Shi, J. Y. Tsang, Y. B. Ni, S. K. Chan, K. F. Chan and G. M. Tse, "FGFR1 is an adverse outcome indicator for luminal A breast cancers", *Oncotarget*, Vol. 7, pp. 5063-5073, 2016.
- [11] N. Turner and R. Grose, "Fibroblast growth factor signalling: from development to cancer", *Nat. Rev. Cancer*, Vol. 10, pp. 116-129, 2010.
- [12] N. Brooks, E. Kilgour, and P. D. Smith, "Molecular pathways: fibroblast growth factor signaling: a new therapeutic opportunity in cancer", *Clin. Cancer Res.*, Vol. 18, pp. 1855-1862, 2012.
- [13] S. Lemieux and M. K. Hadden, "Targeting the fibroblast growth factor receptors for the treatment of cancer", *Anti-Cancer Agents Med. Chem.*, Vol. 13, pp. 748-761, 2013.
- [14] R. Porta, R. Borea, A. Coelho, S. Khan, A. Araújo, P. Reclusa, T. Franchina, N. V. D. Steen, P. V. Dam, J. Ferri, R. Sirera, A. Naing, D. Hong, and C. Rolfo, "FGFR a promising druggable target in cancer: Molecular biology and new drugs", *Crit. Rev. Oncol. Hematol.*, Vol. 113, pp. 256-267, 2017.
- [15] H. Izzedine, S. Ederhy, F. Goldwasser, J. C. Soria, G. Milano, A. Cohen, D. Khayat, and J. P. Spano, "Management of hypertension in angiogenesis inhibitor-treated patients", *Ann. Oncol.*, Vol. 20, pp. 807-815, 2009.
- [16] S. Ricciardi, S. Tomao, and F. de Marinis, "Toxicity of targeted therapy in non-small-cell lung cancer management", *Clin. Lung Cancer*, Vol. 10, pp. 28-35, 2009.
- [17] B. Zhao, Y. Li, P. Xu, Y. Dai, C. Luo, Y. Sun, J. Ai, M. Geng, and W. Duan, "Discovery of substituted 1H-Pyrazolo[3,4-b]pyridine derivatives as potent and selective FGFR kinase inhibitors", *ACS Med. Chem. Lett.*, Vol. 7, pp. 629-634, 2016.
- [18] M. Clark, R. D. Cramer III, and N. V. Opdenbosch, "Validation of the General Purpose Tripos 5.2 Force Field", *J. Comput. Chem.*, Vol. 10, pp. 982-1012, 1989.
- [19] R. Kumar, B. Långström, and T. Darreh-Shori, "Novel ligands of Choline Acetyltransferase designed by in silico molecular docking, hologram QSAR and lead optimization", *Sci. Rep.*, Vol. 6, p. 31247, 2016.
- [20] A. Balupuri, P. K. Balasubramanian, and S. J. Cho, "A CoMFA study of glycogen synthase kinase 3 inhibitors", *J. Chosun Natural Sci.*, Vol. 8, pp. 40-47, 2015.
- [21] A. Balupuri, P. K. Balasubramanian, and S. J. Cho,

- “A CoMFA study of quinazoline-based anticancer agents”, *J. Chosun Natural Sci.*, Vol. 8, pp. 214-220, 2015.
- [22] A. Balupuri, P. K. Balasubramanian, and S. J. Cho, “Comparative molecular field analysis of pyrrolopyrimidines as LRRK2 kinase inhibitors”, *J. Chosun Natural Sci.*, Vol. 9, pp. 1-9, 2016.
- [23] P. K. Balasubramanian, A. Balupuri, and S. J. Cho, “A CoMFA study of phenoxypyridine-based JNK3 inhibitors using various partial charge schemes”, *J. Chosun Natural Sci.*, Vol. 7, pp. 45-49, 2014.